Ultrasound in Med. & Biol., Vol. 41, No. 9, pp. 2400–2411, 2015

0301-5629/$ - see front matter

http://dx.doi.org/10.1016/j.ultrasmedbio.2015.05.004

● *Original Contribution*

RADIOFREQUENCY ABLATION FOR HEPATOCELLULAR CARCINOMA: UTILITY OF CONVENTIONAL ULTRASOUND AND CONTRAST-ENHANCED ULTRASOUND IN GUIDING AND ASSESSING EARLY THERAPEUTIC RESPONSE AND SHORT-TERM FOLLOW-UP RESULTS

JING DU,* HONG-LI LI,* BO ZHAI,† SAMUEL CHANG,‡ and FENG-HUA LI*

* Department of Ultrasound, Renji Hospital, School of Medicine, Shanghai Jiao Tong University, Shanghai, China; † Department of Interventional Oncology, Renji Hospital, School of Medicine, Shanghai Jiao Tong University, Shanghai, China; and ‡ Department of Radiology, University of Colorado Hospital, University of Colorado School of Medicine, Aurora, Colorado, USA

(*Received* 11 *November* 2014; *revised* 28 *April* 2015; *in final form* 4 *May* 2015)

Abstract—The purpose of this study was to assess the efficacy of conventional ultrasound (US) and contrast-enhanced ultrasound (CEUS) in guiding and assessing early therapeutic response to radiofrequency (RF) ablation for hepatocellular carcinomas (HCCs; up to 3 lesions, each ≤3 cm in diameter) and to report the short-term follow-up results. Between September 2011 and January 2013, 63 patients with 78 HCCs (≤3 cm) underwent conventional US- and CEUS-guided percutaneous RF ablation. CEUS was repeated after 20–30 min to assess therapeutic response, and local efficacy was further confirmed by contrast-enhanced magnetic resonance imaging (MRI) 1 mo after tumor ablation. Patients were followed periodically to look for local tumor or disease progression. Survival probability was estimated with the Kaplan–Meier method. Complete ablation was achieved for 76 (97.4%) of 78 HCCs in one (n = 73) or two (n = 3) sessions. No major complications were observed in any patient. The overall concordance in assessment of therapeutic efficacy of RF ablation between CEUS and MRI was 97.4% (76/78 tumors). The concordance test gave a value of $\kappa = 0.74$ ($p < 0.001$), indicating that CEUS had a high diagnostic agreement with MRI. During a mean follow-up of 20 mo, the local tumor progression rate was 5.3% (4/76 tumors). The 1-, 1.5- and 2-y cumulative survival rates were 98.4%, 96.1% and 92.6%, respectively. Although CEUS has some intrinsic limitations, the combined use of conventional US and CEUS provides a safe and efficient tool to guide RF ablation for HCCs 3 cm or smaller, with encouraging results in terms of survival rate and minimal complications. Moreover, the immediate post-procedural CEUS can be a reliable alternative to contrast-enhanced MRI for assessing the early therapeutic response to RF ablation. (E-mail: fenghua-li@163.com and renjizhaibo@163.com) **© 2015 World Federation for Ultrasound in Medicine & Biology.**

Key Words: **Hepatocellular carcinoma, Liver, Radiofrequency ablation, Contrast-enhanced ultrasound, Therapeutic response.**

INTRODUCTION

Radiofrequency (RF) ablation is a safe and effective local treatment option for patients with hepatocellular carcinoma (HCC; Lee et al. 2014). Some studies have even advocated that percutaneous RF ablation can be used successfully as a first-line treatment modality for early-stage HCC (Choi et al. 2007; Kim et al. 2013b; Lee et al. 2014). Although RF ablation can provide potentially curative results for HCC, the procedure is intrinsically dependent on imaging for its planning and assessment of the final outcome. For guiding RF ablation of HCC, various imaging modalities, including ultrasound (US), computed tomography (CT) and magnetic resonance imaging (MRI), can be used (Goldberg et al. 2009). Among them, conventional gray-scale US has been the most widely used guiding modality, thanks to its easy accessibility, low cost, real-time imaging capability and no radiation hazard to the patients. However, not all HCCs are suitable for conventional gray-scale US-guided RF ablation. For

Address correspondence to: Feng-Hua Li, Department of Ultrasound, Renji Hospital, School of Medicine, Shanghai Jiao Tong University, 160 Pujian Rd, Shanghai 200127, China. E-mail: fenghua-li@163.com and Bo Zhai, Department of Interventional Oncology, Renji Hospital, School of Medicine, Shanghai Jiao Tong University, 160 Pujian Rd, Shanghai 200127, China. E-mail: renjizhaibo@163.com

example, some HCCs less than or equal to 3 cm are often less conspicuous due to either their isoechoic nature and/or their locations in the sonographic blind spots such as the liver dome (Lee et al. 2010). In addition, the identification of target lesions is also difficult when the true HCC nodules must be distinguished from many large regenerative nodules in a cirrhotic liver (Minami et al. 2004). Therefore, accurate detection and localization of the true index tumor is essential for successful local ablation treatment of HCCs 3 cm or smaller.

Implementation of contrast-enhanced US (CEUS) can be helpful to enhance the technical feasibility of US-guided RF ablation of HCCs, and it has various advantages in guiding ablation procedure and assessing the therapeutic efficacy (Minami and Kudo 2011; Meloni et al. 2006; Solbiati et al. 2004). CEUS provides a relatively longer time window to the operator to perform RF ablation, allows real-time visualization, can be used in patients with compromised renal function, and has been shown to be a further option to contrast-enhanced CT and MRI for assessing therapeutic response (Frieser et al. 2011; Rajesh et al. 2013). Moreover, CEUS is especially helpful for localizing the index tumors with poor sonographic conspicuity during percutaneous US-guided RF ablation of HCCs (Minami et al. 2004; Minami and Kudo 2011; Rajesh et al. 2013). However, for HCCs 3 cm or smaller, applying CEUS to a RF ablation procedure is still difficult since some tumors do not show typical enhancement characteristics and deep-seated small lesions are easily missed on CEUS due to attenuation of the US beam (Gaiani et al. 2004; Kim et al. 2013a). The combined use of conventional gray-scale US and CEUS might achieve the advantage complementation of two modalities to guide RF ablation. In terms of the post-procedural assessment, the early and accurate evaluation of tumoral response to ablation therapy using imaging modalities is important for determining whether the tumor is completely treated or needs additional treatment (Kim et al. 2005; Sparchez et al. 2009). Having an excellent accuracy in depicting the micro-vascularization of an HCC nodule, CEUS has been used to detect residual tumor immediately after the RF ablation (Gallotti et al. 2009; Meloni et al. 2012; Sparchez et al. 2009). Even though many previous clinical trials documented local response rate and various clinical results of RF ablation (Choi et al. 2007; Kim et al. 2013a; Mazzaferro et al. 2004; Pompili et al. 2013), there have been few reports that focused on combined conventional US- and CEUS-guided percutaneous RF ablation for HCCs 3 cm or smaller and early assessment of therapeutic response with CEUS.

The purpose of our study, therefore, was to assess the efficacy of the combined use of conventional US and CEUS in guiding percutaneous RF ablation for HCC (up to three lesions, each ≤3 cm), and to determine the utility of CEUS in the early assessment of therapeutic response to RF ablation. The short-term follow-up results were also reported in the evaluation of post-ablation complications, the local tumor progression rate and survival rates of patients.

MATERIAL AND METHODS

Patient population

This prospective study was approved by the institutional review board, and written informed consent was obtained from all patients before imaging examinations and ablation procedures. All the patients underwent dynamic contrast-enhanced MRI within 1 mo prior to RF ablation treatment to assess the location, number and size of the tumors. Inclusion criteria for this study were (i) up to 3 lesions per patient; (ii) maximum tumor diameter smaller than or equal to 3 cm; (iii) lesion located at least 3 mm away from the main, right or left portal vein and the gallbladder; and (iv) Child–Pugh class A or B liver cirrhosis, prothrombin time ratio >50% and platelet count >50,000/μL. Lesions with a large exophytic component, adjacent organ or bowel invasion or associated tumor thrombosis of the portal vein or extra-hepatic metastases were excluded. The lesions that could not be detected by both conventional US and CEUS were excluded and had to switch to an alternate guiding method to complete the ablation procedure. The lesions with lack of at least 10 mo follow-up contrast-enhanced MRI were also excluded from our study. The diagnosis of HCC was based on the typical imaging features (arterial phase hyper-enhancement followed by portal venous or delayed phase washout) of the dynamic contrast-enhanced CT and/or MRI or biopsy (Bruix et al. 2011).

Between September 2011 and January 2013, 76 patients with 93 HCCs 3 cm or smaller were enrolled consecutively in this study. Four of the 76 patients were excluded from the study population because their four HCC nodules could not been detected by both conventional US and CEUS as a result of coarse parenchymal echotexture of a cirrhotic liver and poor sonic window associated with shrunken liver volume. A total of 72 patients with 89 HCCs underwent conventional gray-scale US and CEUS-guided percutaneous RF ablation. Nine patients with 11 tumors were excluded who did not have the required follow-up contrast-enhanced MRI following RF ablation treatment; within 10 mo after tumor ablation, only one or two times follow-up contrast-enhanced MRIs were performed in these nine patients, and then they were lost to

Table 1. Baseline features of the study population

Clinical features	Values
Age (y)	
Mean ± SD (range)	55 ± 7 (41–67)
Sex	
Male, n (%)	55 (87.3)
Female, n (%)	8 (12.7)
AFP (ng/mL)	
Median (range)	139.8 (3.3–2147.6)
Previous treatment	
Liver resection, n (%)	45 (71.4)
RF ablation, n (%)	10 (15.9)
Chemotherapy, n (%)	1 (1.6)
Microwave ablation, n (%)	1 (1.6)
Liver resection and transarterial chemoembolization or RF ablation, n (%)	6 (9.5)
Etiology of liver disease	
Hepatitis B virus, n (%)	54 (85.7)
Hepatitis C virus, n (%)	3 (4.8)
Alcohol, n (%)	2 (3.2)
Alcohol and Hepatitis B virus, n (%)	4 (6.3)
Diagnosis of HCC	
Imaging criteria, n (%)	29 (46.0)
Histopathology, n (%)	34 (54.0)
Tumor number	
Single, n (%)	51 (81.0)
Two, n (%)	9 (14.3)
Three, n (%)	3 (4.8)
Tumor size, (cm)	
Mean ± SD (range)	1.5 ± 0.4 (0.8–2.9)

SD = standard deviation; AFP = alpha-foetoprotein; RF = radiofrequency; HCC = hepatocellular carcinoma.

follow-up. Therefore, 63 patients (55 men and 8 women; mean age, 55 y; range, 41–67 y) with 78 HCCs 3 cm or smaller were included in our cohort. Baseline features of the study population are summarized in Table 1. Fifty-one patients had a history of surgical resection of primary HCC and one or more new HCC lesions developed in other parts of the liver on follow-up scans. Therefore, they refused re-operation and selected RF ablation therapy because of minor injury and much lower cost. The remaining 12 patients who had undergone RF ablation, microwave ablation or chemotherapy selected further RF ablation therapy for new hepatic tumors due to their weak physical conditions or the lack of a suitable donor liver for transplantation. For these patients, RF ablation was able to control tumor progression without additional complications and acted as an effective bridge to transplantation. In this study, 37 liver nodules in 29 patients were considered as HCC by means of characteristic imaging findings. The remaining 41 liver lesions in 34 patients were confirmed as HCC by US-guided percutaneous fine-needle biopsy, as non-invasive diagnostic criteria were not satisfied. The underlying causes of liver disease were as follows: Hepatitis B virus in 54 patients, hepatitis C virus in three and alcoholic liver disease in two, while in four patients alcoholic liver disease was associated with hepatitis B virus. Furthermore, 51 patients had a single nodule, nine had two nodules and three patients had three nodules on imaging examinations.

Pre-treatment US examinations

Conventional gray-scale US and CEUS examinations were performed using a Sequoia 512 scanner (Acuson-Siemens, Erlangen, Germany) equipped with a 4 V1 vector transducer (frequency range, 1.0–4.0 MHz). Contrast pulse sequencing (CPS), a contrast-specific imaging modality, was used at a low mechanical index (0.15) level. The low acoustic power enabled maximum preservation of microbubbles in the circulation, thereby making prolonged real-time scanning possible. The US contrast agent used was sulfur hexafluoride-filled microbubbles (SonoVue; Bracco SpA, Milan, Italy), which was supplied as a lyophilized powder and reconstituted with 5 mL of saline solution to form a homogeneous micro-bubble suspension. Each injection was given as 1.5 mL of contrast agent *via* the antecubital vein in a bolus fashion through a 20-gauge intravenous cannula within 1–2 s, followed by a flush with 5 mL of 0.9% normal saline solution. When the lesion began to show enhancement, the patients were asked to hold their breath. The CPS mode was initiated for contrast imaging studies, and the lesion was observed continuously for 5 min. For the patients with two or three suspicious nodules, the pre-treatment CEUS examination was performed on each nodule by repeated bolus injections of SonoVue.

All conventional US and three-phase CEUS examinations were performed by an investigator (J.D.) with 6 y of experience in CEUS. Before intravenous bolus injection of the contrast agent, the liver was scanned by fundamental gray-scale imaging to determine the location, number, size and margin of the index tumor. CEUS using the dual-imaging mode (*i.e.,* simultaneous side-by-side display of gray-scale and contrast-specific mode) was performed in all patients to further determine the actual lesion region and ablation scope. Smaller HCCs not optimally visualized on gray-scale US were located referring to anatomic position on multiphasic contrast-enhanced CT or MRI. At the appearance of the first micro-bubble signal in the liver parenchyma, the patients were requested to hold their breath. Real-time images in the optimal scanning plane were displayed by slightly changing the scanning slice showing the HCC nodules. Conventional ultrasonographic images and the whole CEUS process were stored on the hard disk incorporated in the scanner. All US images and video clips of the 63 patients with HCC were analyzed by two other investigators (H.L.L. and F.H.L.) with 7 and 9 y of experience in CEUS, respectively, who had not performed the conventional US and CEUS examinations and were blinded to other imaging findings. Initially, each reader independently performed the assessment of index tumors, including the number, size and margin of HCC lesions before and after injection of SonoVue; echo patterns (hypo-echoic, isoechoic, or hyper-echoic); and contrast enhancement patterns (hyper-vascularity or hypo-vascularity in the arterial phase, with or without washout of the contrast agent in the portal venous and/or delayed phase). Subsequently, two readers jointly reviewed the images of which they originally had different opinions and then came to a consensus on the characterization of HCC lesions in those cases.

Ablation procedure

RF ablation was performed with a 150-W Model S-1500 RF Generator (MedSphere International, Shanghai, China) and MSI SA Electrodes (MedSphere International, Shanghai, China) with eight curved deployable tines and an active trocar tip for uniform ablation of lesions ranging from 1 to 4 cm. The ablation procedure was done under local anesthesia with or without conscious sedation. Local anesthesia was induced by injecting 5 mL of 1% lidocaine into the abdominal wall from the skin to the peritoneum along a pre-determined puncture line before ablation. Conscious sedation was performed in 23 patients by giving 0.05 mg/kg midazolam and 3 μg/kg fentanyl while the cardiovascular and respiratory systems were continuously monitored.

When the index tumors could be identified on conventional gray-scale US, the RF ablation probe was introduced under conventional US guidance, the electrode tines were deployed according to the size of the lesion and ablation was performed. During RF ablation, only the patients with HCC nodules not clearly depicted on gray-scale US underwent a second CEUS examination, and the RF ablation probe was introduced under three-phase CEUS guidance. Dual-imaging mode was used to reduce the disturbance of a strong increase of the echogenicity and the artifacts because during the ablation procedure the conspicuity of the ablation zone was better on the gray-scale image than on the CEUS image. The generator was set in the impedance mode and RF power was increased in 10-W increments per min from 30 W until it reached the preset maximum power of 100 W or it impeded out. During RF ablation, a hyper-echoic zone was observed around the electrode tip on ultrasonic real-time monitoring. Up to three applications of RF were given in the treatment session so that this hyper-echoic zone covered a larger area than the HCC. Needle tract ablation was also performed while withdrawing the probe. All RF ablation procedures were performed percutaneously by a single interventionalist (B.Z.) with 12 y of experience in US-guided interventional procedures. CEUS was repeated 20–30 min after the ablation to look for any residual arterial phase enhancement and to assess the adequacy of ablation. Complete ablation was considered achieved when there was no enhancing portion within or at the margin of the ablated tumor during the hepatic arterial phase and the ablation zone extended 0.5 to 1 cm beyond the index tumor border. Incomplete ablation was defined as a portion of treated HCC showing persistent hyper-vascularity in the arterial phase, usually appearing as an irregular or peripheral nodular enhancement in the ablation zone. When there were suspicious residual lesions on CEUS, the patients underwent immediate follow-up contrast-enhanced MRI. In cases of incomplete ablation, additional RF ablation was performed with a corrected electrode position and evaluated again using CEUS. This procedure was repeated until a complete ablation was achieved. Immediately after RF ablation, all patients were evaluated by US examinations to ascertain whether any immediate complications such as active bleeding had occurred, and then the patients were observed overnight and discharged the following d after the ablation.

Follow-up protocol

Contrast-enhanced MRI was performed at 1 mo after tumor ablation to assess the therapeutic response and every 3 mo thereafter to look for tumor progression. Therapeutic response was evaluated according to the modified Response Evaluation Criteria In Solid Tumors (Lencioni and Llovet 2010). Complete response was defined as the disappearance of any intra-tumoral arterial enhancement in the target lesion. Residual tumor was defined as an arterial phase-enhancing lesion within or surrounding the RF ablation zone. Local tumor progression was determined when a subsequent follow-up MRI demonstrated any growing and enhancing tumor within or at the margin of the ablation zone, where there had been complete primary effectiveness. New HCC was defined as an intra-hepatic tumor showing the characteristic enhancement pattern of HCC outside the RF ablation zone.

All patients were followed monthly with physical examination, liver function tests and AFP measurement in the first 6 mo after treatment, and thereafter at 3–6 mo intervals. Survival analysis was performed on patient basis. The overall survival time was defined as the interval between the first RF ablation and either death or the last follow-up contact for patients by December 30, 2013.

Statistical analysis

The Student's *t*-test was applied to evaluate the tumor size discrepancy between conventional US and CEUS. The results of CEUS in assessment of therapeutic efficacy were compared with those of MRI by the concordance test. Survival probability was estimated by Kaplan–Meier method. A p value of <0.05 was considered statistically significant. All statistical analyses were performed using SPSS software version 13.0 (SPSS Inc; Chicago, IL, USA).

RESULTS

Pre-treatment US findings

Among 63 patients, a total of 78 HCCs 3 cm or smaller (mean 1.5 cm, range 0.8–2.9 cm in diameter) were ablated under the guidance of conventional gray-scale US and CEUS. Pre-treatment conventional US and CEUS findings are presented in Table 2. On conventional gray-scale US, all the lesions appeared as solid nodules with different sonographic patterns. Of the 78 HCCs 3 cm or smaller, 57 (73.1%) were hypo-echoic, 18 (23.1%) were isoechoic and three (3.8%) were hyper-echoic. Moreover, 54 (69.2%) of 78 HCCs were smaller than 2 cm in maximum diameter. Of these 54 small HCCs, 41 (75.9%) were hypo-echoic, 12 (22.2%) were isoechoic and one (1.9%) was hyper-echoic. Peripheral hypo-echoic halos were seen in 6 (7.7%) isoechoic or hyper-echoic nodules. The 18 (23.1%) isoechoic nodules not clearly depicted on gray-scale US were detected by CEUS scan. In addition, the shape and border of 27 (34.6%) HCC nodules with ill-defined margins on conventional gray-scale US could be well visualized on CEUS. The size of 20 (25.6%) HCCs measured at the artery phase of CEUS appeared larger compared to those obtained from conventional gray-scale US (1.8 $\pm$ 0.5 cm vs 1.5 $\pm$ 0.4 cm; $p = 0.03$). In three patients with multifocal HCC lesions, pre-treatment contrast-enhanced MRI had identified all the hepatic tumors. By referring to the findings on contrast-enhanced MRI and repeated injections of contrast medium, CEUS detected multifocal tumor lesions in advanced liver cirrhosis and identified the true HCC nodules, which could not be differentiated from many large regenerative nodules at conventional gray-scale US (Fig. 1).

As shown in Table 2, 36 (46.2%) of the 78 HCCs showed a typical enhancement pattern on CEUS—hyper-vascularity in the arterial phase with washout of the contrast agent in the portal venous and/or delayed phase, 34 (43.6%) exhibited only the marked arterial phase hyper-enhancement without obvious washout of contrast agent from lesions and no arterial hyper-vascularization was observed in the remaining eight (10.3%) nodules, though they were hyper-vascular on contrast-enhanced CT or MRI before RF ablation.

Table 2. Conventional US and CEUS findings of the 78 HCC nodules

US findings	No.	%
Internal echo		
Hypo-echoic	57	73.1
Iso-echoic	18	23.1
Hyper-echoic	3	3.8
Margin type		
Well-defined	51	65.4
Ill-defined	27	34.6
Peripheral hypo-echoic halo		
Present	6	7.7
Absent	72	92.3
Size discrepancy between two measurements		
Larger	20	25.6
Un-changed	58	74.4
CEUS pattern		
Arterial phase hyper-enhancement and portal venous/delayed phase washout	36	46.2
Only arterial phase hyper-vascularization	34	43.6
No arterial phase hyper-vascularization	8	10.3

US = ultrasound; CEUS = contrast-enhanced ultrasound.

US-guided RF ablation for HCC

Among 78 HCCs 3 cm or smaller, 60 (76.9%) could be visualized on conventional gray-scale US. Of these 60 nodules, 52 nodules displaying arterial phase hyper-enhancement on CEUS were ablated under the guidance of conventional gray-scale US. For these 52 nodules, CEUS was only performed for pre-treatment evaluation of the index tumor and was not performed for real-time guidance of an electrode placement. The other eight nodules showed no arterial hyper-enhancement. During the portal venous phase and delayed phase, the majority (6/8, 75.0%) of nodules without arterial hyper-vascularity on CEUS, were iso-enhanced, while the remaining two nodules were slightly hypo-enhanced in comparison to the surrounding parenchyma. On conventional gray-scale US, five (62.5%) of the eight nodules were located deeply in the posterior segments of the right hepatic lobe ($\geq$9 cm from the transducer), and six (75.0%) were smaller than 2.0 cm in maximum diameter. These eight (10.3%) nodules without arterial hyper-vascularity were targeted and ablated under the guidance of conventional gray-scale US alone (Fig. 2). The remaining 18 (23.1%) nodules were targeted and ablated under the guidance of three-phase CEUS alone as the lesions were not clearly visible on conventional gray-scale US (Fig. 3).

CEUS for the early assessment of therapeutic response

CEUS was repeated 20–30 min after completion of the ablation. CEUS suggested that 75 (96.2%) of the 78 HCCs 3 cm or smaller were completely ablated, and the remaining three (3.8%) were not successfully treated with RF ablation. A second RF ablation session was performed after these three residual un-ablated tumors were identified by immediate post-RF ablation MRI. No major post-procedural complications were observed in

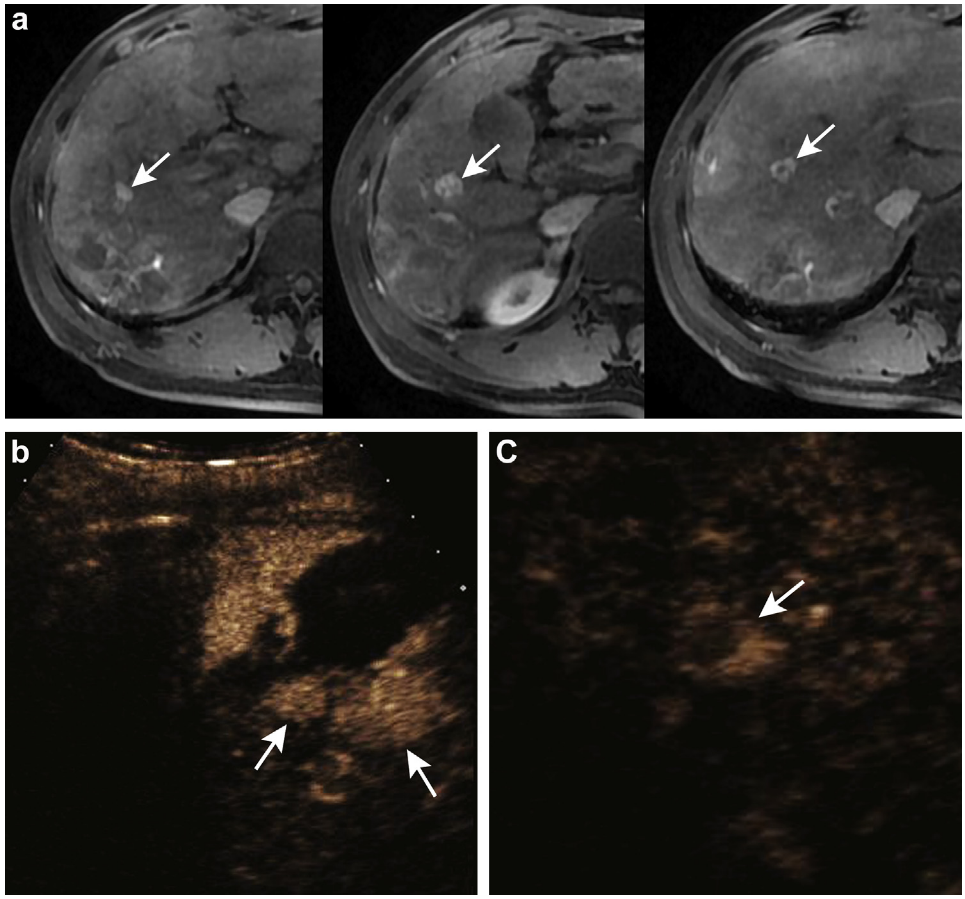

Fig. 1. Multifocal hepatocellular carcinoma (HCC) lesions in a 52-y-old man. (a) Contrast-enhanced MRI performed during the arterial phase shows multifocal viable tumor lesions (arrows) among many large regenerative nodules in advanced cirrhotic liver. (b, c) Before the RF ablation, contrast-enhanced ultrasound (CEUS) images obtained during the arterial phase identify the true HCC nodules (arrows).

any patient. Minor complications, in the form of self-limiting intraperitoneal bleeding, were seen in three (4.8%) of the 63 patients.

Follow-up

Contrast-enhanced MRI scans 1 mo after RF ablation revealed a total of 76 (97.4%) HCCs were completely ablated, whereas the remaining two (2.6%) were not successfully treated with RF ablation (Fig. 4). Thus, five HCCs with poor conspicuity on conventional gray-scale US were not successfully ablated in the first session, and technical effectiveness was achieved for 76 HCCs in one (n = 73) or two (n = 3) RF ablation sessions. The overall concordance in assessment of therapeutic efficacy between CEUS and MRI was 97.4% (76/78 tumors). The concordance test gave a value of the coefficient $\kappa = 0.74$ ($p < 0.001$), indicating a high concordance between the results obtained with CEUS and those obtained with MRI. In our study, immediate post-procedural CEUS performed within 20–30 min after RF ablation showed a sensitivity of 60% (three of five tumors) and a specificity of 100% (73 of 73 tumors) for detection of unsuccessfully treated lesions.

During a mean follow-up of 20 mo (range: 11–29 mo), local tumor progression was identified in four (5.3%) of the 76 ablated tumors with complete primary effectiveness. One or more new lesions developed in other parts of the liver on follow-up scans in 25 (39.7%) of the 63 patients. Four (6.3%) patients died of tumor progression (n = 2), liver failure (n = 1) or complications of cirrhosis (n = 1) within the follow-up. In our study, survival probability for patients with HCC treated with RF ablation was estimated by Kaplan–Meier method. As illustrated in Figure 5, the Kaplan–Meier plot showed the cumulative survival rates at 1, 1.5 and 2 y were 98.4%, 96.1% and 92.6%, respectively.

DISCUSSION

The success rate of RF ablation depends on precise targeting of the lesion under imaging guidance. However,

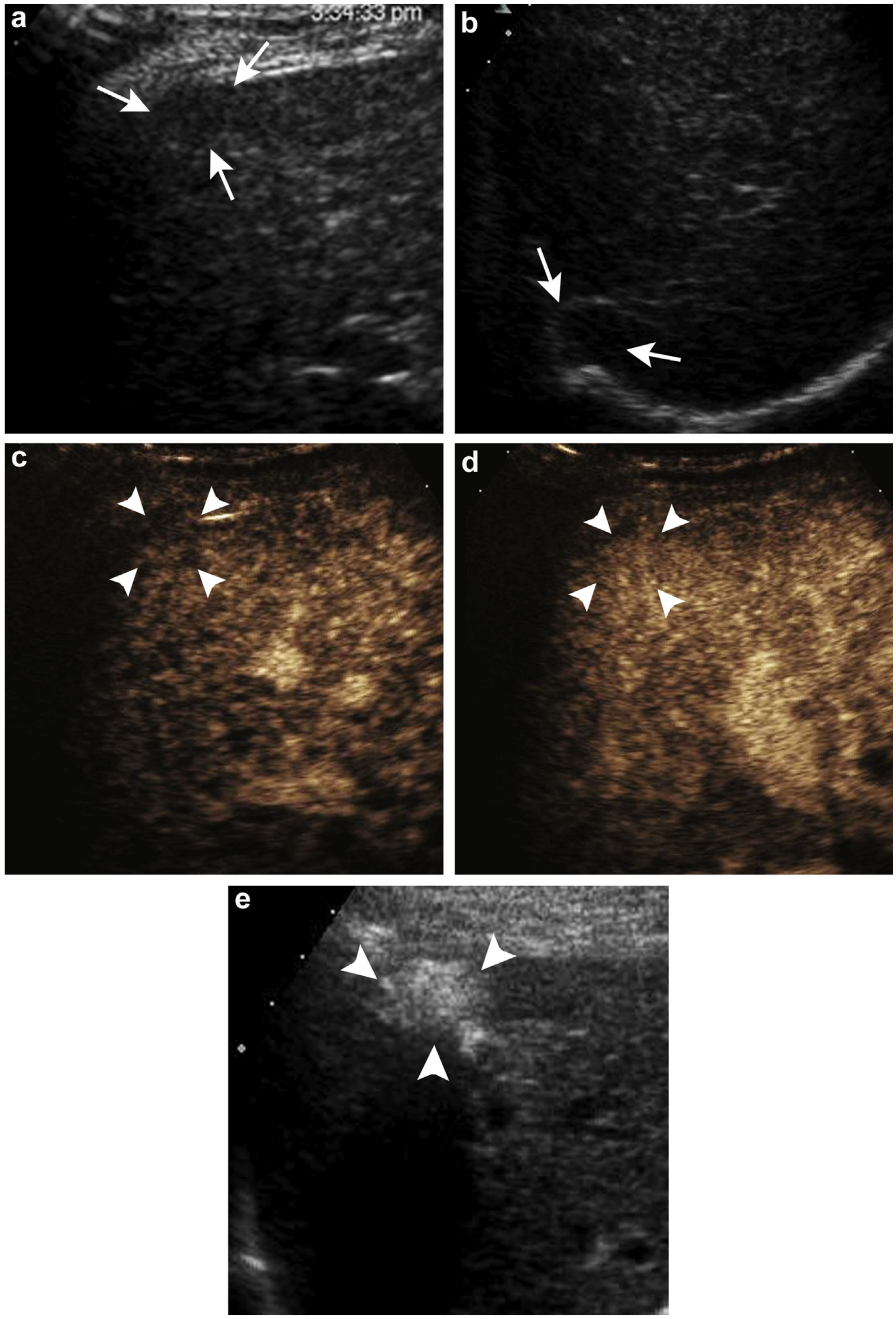

Fig. 2. Radiofrequency (RF) ablation treatment for biopsy-confirmed small hypo-vascular hepatocellular carcinoma (HCC) under conventional gray-scale ultrasound (US) guidance in a 50-y-old man. (a, b) Inter-costal and sub-costal oblique gray-scale US scans show a 1.9-cm oval hypo-echoic lesion in liver segment VIII (arrows). (c, d) The inter-costal contrast-enhanced (CEUS) image shows the nodule (arrowheads) is not visualized in the hepatic arterial phase (31 s) and portal venous phase (48 s) due to iso-enhancement relative to the surrounding liver tissues, and the same CEUS manifestation is also seen in the sub-costal oblique plane (not shown). (e) Hypo-vascular HCC lesion is ablated under the guidance of conventional gray-scale US alone, and inter-costal gray-scale US scan immediately after the ablation shows a hyper-echoic ablation zone (arrowheads) completely covering the index tumor.

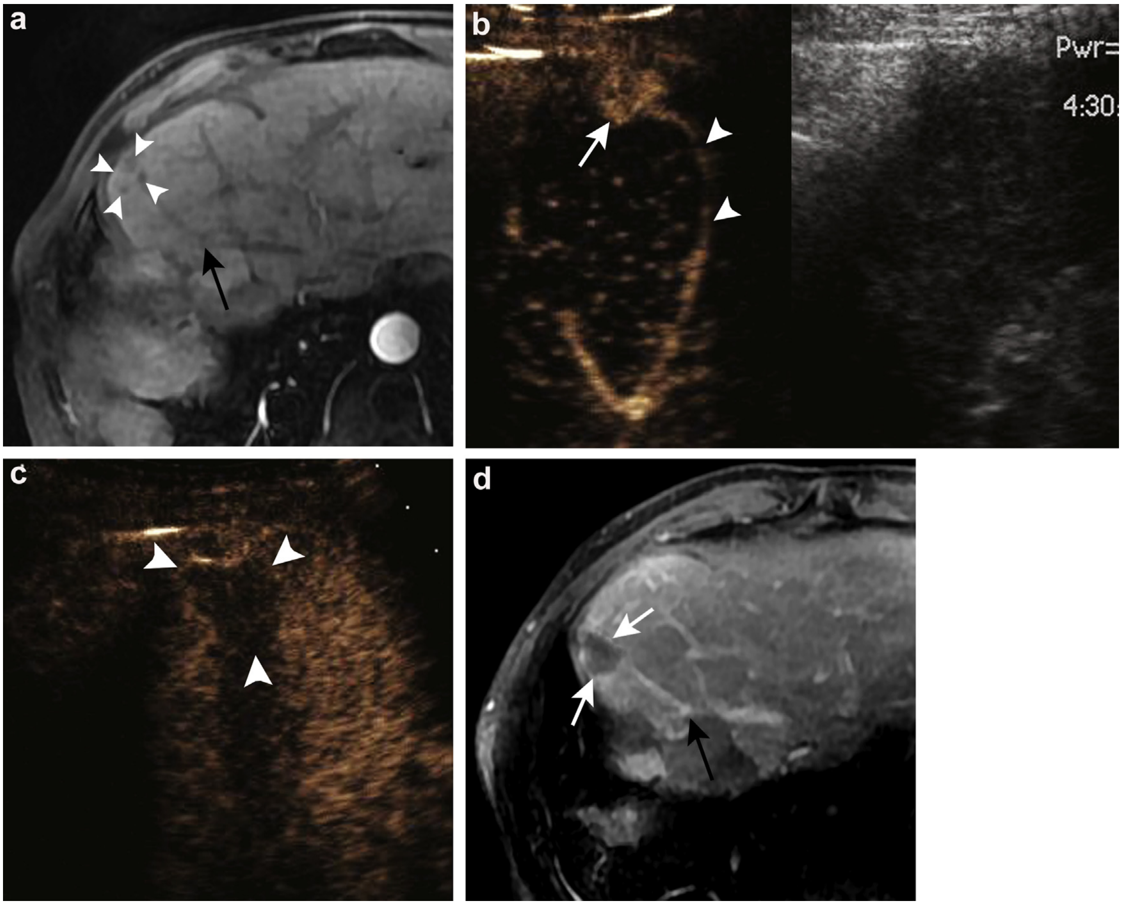

Fig. 3. Biopsy-confirmed small isoechoic hepatocellular carcinoma (HCC) before and after successful radiofrequency (RF) ablation in a 64-y-old-man. (a) Contrast-enhanced MRI performed before RF ablation shows an ill-defined heterogeneous iso-enhancing nodule (arrowheads) in liver segment VIII, which presents with multiple small hypo-enhancing areas. (b) A 1.5-cm heterogeneous hyper-enhancing nodule (arrow) is shown on arterial phase contrast-enhanced ultrasound (CEUS) image, whereas this lesion could not be visualized on gray-scale US. One feeding vessel (arrowheads) that enters the lesion's periphery is detected by CEUS. (c) After RF ablation, CEUS image obtained 27 s after contrast agent injection shows no vascularity within the ablation zone (arrowheads). (d) The diagnosis of complete necrosis (arrows) is confirmed by 1-mo post-ablation contrast-enhanced MRI. The same feeding vessel (black arrow) entering the lesion's periphery could also be seen on MRI images (a and d), suggesting that the anatomic location of the index tumor is consistent with the ablation zone.

visualization of a lesion on conventional gray-scale US is difficult at times as a result of coarse parenchymal echotexture of a cirrhotic liver and poor sonic window associated with shrunken liver volume. Our study showed that only 76.9% of HCCs 3 cm or smaller were visible on pre-ablation planning gray-scale US performed with known CT or MRI results, which was consistent with the previously published literature (Kim et al. 2012). Although contrast-enhanced CT or MRI-guided RF ablation has been shown to be potentially useful for the treatment of HCC nodules that are not visualized by gray-scale US, real-time visualization is inferior to US guidance, and sometimes the procedures are accompanied by radiation exposure to patients and operators (Masuzaki et al. 2011; Rajesh et al. 2013). The results of our study have demonstrated that the use of pre-ablation CEUS is very helpful for localizing HCC nodules not well visualized by gray-scale US and can clearly depict the shape and boundary of HCC lesions with ill-defined margins. During the RF ablation procedures, CEUS significantly helped real-time guidance of RF ablation for HCC lesions that could not be adequately depicted at gray-scale US, which was in agreement with the findings of previous studies (Dong et al. 2014; Rajesh et al. 2013). The size of 20 (25.6%) HCCs measured on arterial phase CEUS images appeared significantly larger than those obtained from gray-scale US images, which suggested that a routine use of pre-treatment CEUS examination might reduce the number of incomplete ablations as the safety

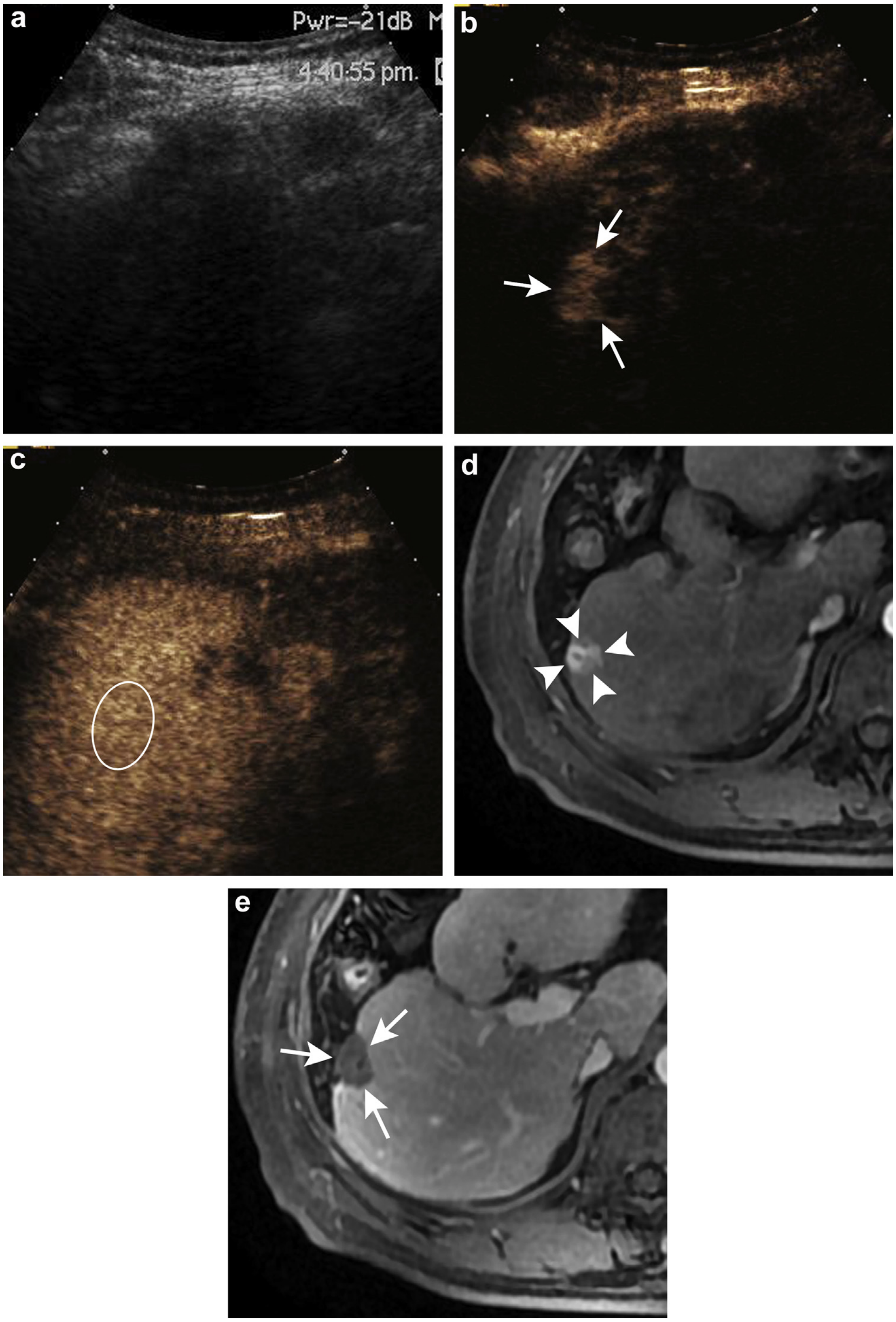

Fig. 4. Small hepatocellular carcinoma (HCC) unsuccessfully treated with radiofrequency (RF) ablation under the contrast-enhanced ultrasound (CEUS) guidance in a 57-y-old man. (a) The HCC nodule could not be clearly visualized on conventional gray-scale ultrasound (US). (b, c) CEUS images in the hepatic arterial phase (26 s) and portal vein phase (48 s) after the injection of microbubbles show a 1.8-cm sized, only transiently hyper-enhanced nodule (arrows) without obvious washout of contrast agent (white ellipse). (d, e) Contrast-enhanced MRI performed 1 mo after CEUS-guided RF ablation shows a deviation of the ablation zone (arrows) close to the index tumor (arrowheads) in liver segment VII.

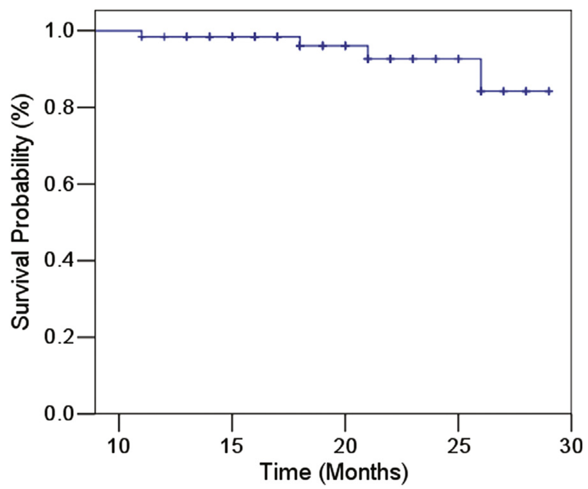

Fig. 5. Graph shows Kaplan–Meier survival estimation for 63 patients who underwent radiofrequency (RF) ablation treatment for hepatocellular carcinomas (HCCs) less than or equal to 3 cm.

margin could be more clearly determined. By referring to anatomic position on pre-ablation contrast-enhanced MRI and repeated injections of contrast medium, CEUS could detect multi-focal tumor lesions and identify the true HCC nodules among many large regenerative nodules in advanced cirrhotic liver.

However, applying CEUS to a RF ablation procedure is not always beneficial because some smaller HCCs do not show typical arterial phase hyper-enhancement and portal venous/delayed phase washout on CEUS. This is more frequently found in HCCs that are well differentiated (Kim et al. 2011b, 2013a). In our study, 34 (43.6%) of the 78 HCCs 3 cm or smaller showed only the arterial hyper-vascularity without obvious washout of contrast agent from lesions. Of these 34 HCCs with only transient hyper-enhancement in arterial phase, 24 (70.6%) were small HCCs less than 2 cm. The temporal window of the arterial phase in which hyper-vascularity can be depicted is sometimes not long enough for real-time monitoring for placement of an electrode. Therefore, real-time targeting under guidance of arterial phase CEUS can be technically difficult and may need an experienced operator. In our study, five HCCs with poor conspicuity on conventional gray-scale US were not successfully ablated in the first session, which might be correlated with their small size, location in the sonographic blind spot, deviation caused by respiratory movements and not enough time for real-time targeting due to only transient hyper-enhancement in arterial phase. CEUS-guided RF ablation with the use of Sonazoid, a kind of shelled perfluorobutane-based US contrast agent, might be helpful in achieving complete RF ablation of these lesions. Compared to SonoVue, Sonazoid could provide a longer temporal window for the interventionalist for the detection, localization and ablation of HCC lesions (Dohmen et al. 2012; Masuzaki et al. 2011). Since 2009, fusion imaging techniques of US and CT/MR images have been shown to be of use in the localization and targeting of HCC nodules that are not visualized by gray-scale US (Lee et al. 2012; Nakai et al. 2009; Song et al. 2013). However, fusion images between US and CT/MRI do not always accurately correspond to the actual US images because of the discrepancies caused by respiratory movements, changes in posture and bowel peristalsis (Rajesh et al. 2013).

When CEUS is used to guide the RF ablation, detection of arterial phase hyper-vascularity is crucial to make a diagnosis of HCC as it is one of the most reliable characteristics of HCC (Jang et al. 2009). However, there is a small subset of HCCs with no arterial phase hyper-vascularity, particularly those that are well differentiated (Jang et al. 2007; Kim et al. 2011b). Moreover, CEUS is slightly less sensitive than contrast-enhanced CT and MRI in the detection of arterial phase hyper-vascularity, especially for very small (≤1 cm in size) or deep-seated lesions (Gaiani et al. 2004; Giorgio et al. 2007). In our study, eight (10.3%) of the 78 HCCs showed no arterial phase hyper-vascularity on CEUS, most of which were small HCC lesions. However, complete ablation was achieved in a single session in these eight tumors under the guidance of conventional gray-scale US alone. This suggests that conventional gray-scale US can provide valuable images to help guide RF ablation therapy for such small HCCs without arterial hyper-vascularity.

The results of our study demonstrated that the overall concordance in post-procedural assessment of therapeutic efficacy of RF ablation between CEUS and contrast-enhanced MRI was 97.4% (76 of 78 tumors), which indicated that CEUS had a high diagnostic agreement with MRI. However, the early assessment of therapeutic response using CEUS is limited by a relatively high rate of false negative results. A previous study demonstrated that immediate post-procedural CEUS performed within 1 h after RF ablation showed poor sensitivity (40%) with relatively high specificity (94%) for detection of residual tumor when CT or MRI results were used as a reference standard (Dill-Macky et al. 2006). In our study, immediate post-procedural CEUS suggested that 75 (96.2%) of the 78 HCCs were completely ablated. A second RF ablation was performed after three residual un-ablated tumors were identified by immediate post-RF ablation MRI. With the findings of 1-mo follow-up contrast-enhanced MRI as the reference standard, immediate CEUS performed within 20–30 min after

RF ablation showed 60% (3 of 5 tumors) sensitivity with 100% (73 of 73 tumors) specificity for detection of unsuccessfully treated lesions. Two un-ablated viable tumors failed to be detected by CEUS, which could be ascribed to the small lesion size, unfavorable locations for observation, the limiting two-dimensional ultrasonic plane and benign reactive enhancement around the RF ablation zone. Although the sensitivity of CEUS in early detection of residual un-ablated tumors was lower, immediate post-procedural CEUS could be of extreme importance allowing retreatment in the same session and, therefore, reducing the number of incomplete ablations.

Conventional US and CEUS have been shown to be efficient imaging modalities in guiding RF ablation of HCC. However, for HCCs less than or equal to 3 cm in diameter, applying either conventional US or CEUS alone to a RF ablation procedure is still difficult due to their isoechoic nature and atypical enhancement patterns. According to previous studies, technical feasibility of US-guided RF ablation for HCCs with mean diameters of 1.8–1.9 cm did not exceed 70% (Kim et al. 2011a, 2013a; Rhim et al. 2008). The results of our study demonstrated that CEUS could enhance the technical feasibility of US-guided RF ablation of HCCs 3 cm or smaller, and has various advantages in pre-treatment evaluation of HCC nodules and real-time guidance of the index tumors with poor sonographic conspicuity. In addition, conventional US could provide valuable images to help guide RF ablation therapy for HCCs with only transient hyper-enhancement in arterial phase or without arterial hyper-vascularity, especially for some small lesions, since not all the small HCCs are isoechoic. Therefore, the combined use of conventional gray-scale US and CEUS might achieve the advantage complementation of two modalities to guide RF ablation. The results of the present study showed that a high complete ablation rate of 97.4% (76/78 tumors) was achieved after one or two sessions under the guidance of conventional US combined with CEUS, with no major procedure-related complications.

Local tumor progression rates for HCCs less than or equal to 3 cm were approximately 10%–20% during the 2–3-y follow-up period (Lin et al. 2005; Shibata et al. 2009). In the present study, the local tumor progression rate was only 5.3% (4/76 tumors) during a mean follow-up of 20 mo (range: 11–29 mo). Lower tumor progression rate might be attributed to several factors, including operators' expertise, tumor location, adequate ablative margin and biologic behavior or histologic grade of the tumor. The cumulative survival rate was higher than 95% at 1 y and 90% at 2 y after RF ablation. However, new lesions developed in other parts of the liver on follow-up scans in 25 (39.7%) of the 63 patients.

This study has several limitations. Firstly, the patients enrolled in this study are numerically small and further studies are needed in a larger patient population to confirm our findings. Secondly, the current results were based on a mean follow-up of 20 mo after RF ablation treatment. A long-term follow-up of these patients to assess local tumor progression rates has yet to be performed. Thirdly, nine patients with 11 tumors were excluded who did not have the required follow-up contrast-enhanced MRI following RF ablation treatment. Appreciable loss to follow-up (9/63; 14.3% of patients) may introduce bias in the estimates of treatment effect. Fourthly, when using CEUS to detect deep-seated smaller lesions, attenuation of the US beam remains an objective limit of this technique. Finally, one limitation of CEUS compared with contrast-enhanced MRI is its lack of panoramicity, *i.e.,* the need to focus analysis on the only one suspect mass, excluding the remaining liver parenchyma. Therefore, the detection of multifocal HCC nodules with CEUS depends on the anatomic location on pre-ablation contrast-enhanced MRI, and repeated injections of contrast medium are also needed.

In conclusion, although CEUS has some intrinsic limitations, the combined use of conventional US and CEUS provides a safe and efficient tool to guide RF ablation for HCCs 3 cm or smaller, with encouraging results in terms of survival rate and minimal complications. In addition, the immediate post-procedural CEUS can be a reliable alternative to contrast-enhanced MRI for assessing the early therapeutic response to RF ablation.

Acknowledgments—The authors would like to acknowledge the financial supports received from the National Natural Science Foundation of China (no. 81102014) and the Training Program for Excellent Young Teachers of Shanghai Jiao Tong University School of Medicine.

REFERENCES

Bruix J, Sherman M, American Association for the Study of Liver Diseases. Management of hepatocellular carcinoma: An update. Hepatology 2011;53:1020–1022.

Choi D, Lim HK, Rhim H, Kim YS, Lee WJ, Paik SW, Koh KC, Lee JH, Choi MS, Yoo BC. Percutaneous radiofrequency ablation for early-stage hepatocellular carcinoma as a first-line treatment: Long-term results and prognostic factors in a large single-institution series. Eur Radiol 2007;17:684–692.

Dill-Macky MJ, Asch M, Burns P, Wilson S. Radiofrequency ablation of hepatocellular carcinoma: predicting success using contrast-enhanced sonography. AJR Am J Roentgenol 2006;186: S287–S295.

Dohmen T, Kataoka E, Yamada I, Miura K, Ohshima S, Shibuya T, Segawa D, Sato W, Anezaki Y, Ishii H, Kamada K, Goto T, Ohnishi H. Efficacy of contrast-enhanced ultrasonography in radiofrequency ablation for hepatocellular carcinoma. Intern Med 2012;51:1–7.

Dong Y, Wang WP, Gan YH, Huang BJ, Ding H. Radiofrequency ablation guided by contrast-enhanced ultrasound for

hepatic malignancies: Preliminary results. Clin Radiol 2014;69: 1129–1135.
Frieser M, Kiesel J, Lindner A, Bernatik T, Haensler JM, Janka R, Hahn EG, Strobel D. Efficacy of contrast-enhanced US versus CT or MRI for the therapeutic control of percutaneous radiofrequency ablation in the case of hepatic malignancies. Ultraschall Med 2011;32:148–153.
Gaiani S, Celli N, Piscaglia F, Cecilioni L, Losinno F, Giangregorio F, Mancini M, Pini P, Fornari F, Bolondi L. Usefulness of contrast-enhanced perfusional sonography in the assessment of hepatocellular carcinoma hypervascular at spiral computed tomography. J Hepatol 2004;41:421–426.
Gallotti A, D'Onofrio M, Ruzzenente A, Martone E, De Robertis R, Guglielmi A, Pozzi Mucelli R. Contrast-enhanced ultrasonography (CEUS) immediately after percutaneous ablation of hepatocellular carcinoma. Radiol Med 2009;114:1094–1105.
Giorgio A, De Stefano G, Coppola C, Ferraioli G, Esposito V, Di Sarno A, Giorgio V, De Stefano M, Sangiovanni V, Liorre G, Del Viscovo L. Contrast-enhanced sonography in the characterization of small hepatocellular carcinomas in cirrhotic patients: Comparison with contrast-enhanced ultrafast magnetic resonance imaging. Anticancer Res 2007;27:4263–4269.
Goldberg SN, Grassi CJ, Cardella JF, Charboneau JW, Dodd GD 3rd, Dupuy DE, Gervais DA, Gillams AR, Kane RA, Lee FT Jr, Livraghi T, McGahan J, Phillips DA, Rhim H, Silverman SG, Solbiati L, Vogl TJ, Wood BJ, Vedantham S, Sacks D. Image-guided tumor ablation: Standardization of terminology and reporting criteria. J Vasc Interv Radiol 2009;20:S377–S390.
Jang HJ, Kim TK, Burns PN, Wilson SR. Enhancement patterns of hepatocellular carcinoma at contrast-enhanced US: Comparison with histologic differentiation. Radiology 2007;244:898–906.
Jang HJ, Kim TK, Wilson SR. Small nodules (1-2 cm) in liver cirrhosis: Characterization with contrast-enhanced ultrasound. Eur J Radiol 2009;72:418–424.
Kim CK, Choi D, Lim HK, Kim SH, Lee WJ, Kim MJ, Lee JY, Jeon YH, Lee J, Lee SJ, Lim JH. Therapeutic response assessment of percutaneous radiofrequency ablation for hepatocellular carcinoma: utility of contrast-enhanced agent detection imaging. Eur J Radiol 2005;56:66–73.
Kim JE, Kim YS, Rhim H, Lim HK, Lee MW, Choi D, Shin SW, Cho SK. Outcomes of patients with hepatocellular carcinoma referred for percutaneous radiofrequency ablation at a tertiary center: Analysis focused on the feasibility with the use of ultrasonography guidance. Eur J Radiol 2011a;79:e80–e84.
Kim PN, Choi D, Rhim H, Rha SE, Hong HP, Lee J, Choi JI, Kim JW, Seo JW, Lee EJ, Lim HK. Planning ultrasound for percutaneous radiofrequency ablation to treat small (≤3 cm) hepatocellular carcinomas detected on computed tomography or magnetic resonance imaging: A multicenter prospective study to assess factors affecting ultrasound visibility. J Vasc Interv Radiol 2012;23:627–634.
Kim TK, Lee KH, Khalili K, Jang HJ. Hepatocellular nodules in liver cirrhosis: Contrast-enhanced ultrasound. Abdom Imaging 2011b; 36:244–263.
Kim YJ, Lee MW, Park HS. Small hepatocellular carcinomas: Ultrasonography guided percutaneous radiofrequency ablation. Abdom Imaging 2013a;38:98–111.
Kim YS, Lim HK, Rhim H, Lee MW, Choi D, Lee WJ, Paik SW, Koh KC, Lee JH, Choi MS, Gwak GY, Yoo BC. Ten-year outcomes of percutaneous radiofrequency ablation as first-line therapy of early hepatocellular carcinoma: Analysis of prognostic factors. J Hepatol 2013b;58:89–97.
Lee DH, Lee JM, Lee JY, Kim SH, Yoon JH, Kim YJ, Han JK, Choi BI. Radiofrequency ablation of hepatocellular carcinoma as first-line treatment: Long-term results and prognostic factors in 162 patients with cirrhosis. Radiology 2014;270:900–909.
Lee MW, Kim YJ, Park HS, Yu NC, Jung SI, Ko SY, Jeon HJ. Targeted sonography for small hepatocellular carcinoma discovered by CT or MRI: Factors affecting sonographic detection. AJR Am J Roentgenol 2010;194:W396–W400.
Lee MW, Rhim H, Cha DI, Kim YJ, Choi D, Kim YS, Lim HK. Percutaneous radiofrequency ablation of hepatocellular carcinoma: Fusion imaging guidance for management of lesions with poor conspicuity at conventional sonography. AJR Am J Roentgenol 2012;198:1438–1444.
Lencioni R, Llovet JM. Modified RECIST (mRECIST) assessment for hepatocellular carcinoma. Semin Liver Dis 2010;30:52–60.
Lin SM, Lin CJ, Lin CC, Hsu CW, Chen YC. Randomised controlled trial comparing percutaneous radiofrequency thermal ablation, percutaneous ethanol injection, and percutaneous acetic acid injection to treat hepatocellular carcinoma of 3 cm or less. Gut 2005;54:1151–1156.
Masuzaki R, Shiina S, Tateishi R, Yoshida H, Goto E, Sugioka Y, Kondo Y, Goto T, Ikeda H, Omata M, Koike K. Utility of contrast-enhanced ultrasonography with Sonazoid in radiofrequency ablation for hepatocellular carcinoma. J Gastroenterol Hepatol 2011;26:759–764.
Mazzaferro V, Battiston C, Perrone S, Pulvirenti A, Regalia E, Romito R, Sarli D, Schiavo M, Garbagnati F, Marchianò A, Spreafico C, Camerini T, Mariani L, Miceli R, Andreola S. Radiofrequency ablation of small hepatocellular carcinoma in cirrhotic patients awaiting liver transplantation: A prospective study. Ann Surg 2004;240:900–909.
Meloni MF, Andreano A, Zimbaro F, Lava M, Lazzaroni S, Sironi S. Contrast enhanced ultrasound: Roles in immediate post-procedural and 24-h evaluation of the effectiveness of thermal ablation of liver tumors. J Ultrasound 2012;15:207–214.
Meloni MF, Livraghi T, Filice C, Lazzaroni S, Calliada F, Perretti L. Radiofrequency ablation of liver tumors: The role of microbubble ultrasound contrast agents. Ultrasound Q 2006;22:41–47.
Minami Y, Kudo M, Kawasaki T, Chung H, Ogawa C, Shiozaki H. Treatment of hepatocellular carcinoma with percutaneous radiofrequency ablation: Usefulness of contrast harmonic sonography for lesions poorly defined with B-mode sonography. AJR Am J Roentgenol 2004;183:153–156.
Minami Y, Kudo M. Review of dynamic contrast-enhanced ultrasound guidance in ablation therapy for hepatocellular carcinoma. World J Gastroenterol 2011;17:4952–4959.
Nakai M, Sato M, Sahara S, Takasaka I, Kawai N, Minamiguchi H, Tanihata H, Kimura M, Takeuchi N. Radiofrequency ablation assisted by real-time virtual sonography and CT for hepatocellular carcinoma undetectable by conventional sonography. Cardiovasc Intervent Radiol 2009;32:62–69.
Pompili M, Saviano A, de Matthaeis N, Cucchetti A, Ardito F, Federico B, Brunello F, Pinna AD, Giorgio A, Giulini SM, De Sio I, Torzilli G, Fornari F, Capussotti L, Guglielmi A, Piscaglia F, Aldrighetti L, Caturelli E, Calise F, Nuzzo G, Rapaccini GL, Giuliante F. Long-term effectiveness of resection and radiofrequency ablation for single hepatocellular carcinoma ≤3 cm. Results of a multicenter Italian survey. J Hepatol 2013;59:89–97.
Rajesh S, Mukund A, Arora A, Jain D, Sarin SK. Contrast-enhanced US-guided radiofrequency ablation of hepatocellular carcinoma. J Vasc Interv Radiol 2013;24:1235–1240.
Rhim H, Lee MH, Kim YS, Choi D, Lee WJ, Lim HK. Planning sonography to assess the feasibility of percutaneous radiofrequency ablation of hepatocellular carcinomas. AJR Am J Roentgenol 2008; 190:1324–1330.
Shibata T, Isoda H, Hirokawa Y, Arizono S, Shimada K, Togashi K. Small hepatocellular carcinoma: Is radiofrequency ablation combined with transcatheter arterial chemoembolization more effective than radiofrequency ablation alone for treatment? Radiology 2009; 252:905–913.
Solbiati L, Ierace T, Tonolini M, Cova L. Guidance and monitoring of radiofrequency liver tumor ablation with contrast-enhanced ultrasound. Eur J Radiol 2004;51(Suppl):S19–S23.
Song KD, Lee MW, Rhim H, Cha DI, Chong Y, Lim HK. Fusion imaging-guided radiofrequency ablation for hepatocellular carcinomas not visible on conventional ultrasound. AJR Am J Roentgenol 2013;201:1141–1147.
Sparchez Z, Radu P, Anton O, Socaciu M, Badea R. Contrast-enhanced ultrasound in assessing therapeutic response in ablative treatments of hepatocellular carcinoma. J Gastrointestin Liver Dis 2009;18: 243–248.